

Local feature point extraction for quantum images

Yi Zhang · Kai Lu · Kai Xu · Yinghui Gao ·
Richard Wilson

Received: 28 May 2014 / Accepted: 20 September 2014 / Published online: 30 September 2014
© Springer Science+Business Media New York 2014

Abstract Quantum image processing has been a hot issue in the last decade. However, the lack of the quantum feature extraction method leads to the limitation of quantum image understanding. In this paper, a quantum feature extraction framework is proposed based on the novel enhanced quantum representation of digital images. Based on the design of quantum image addition and subtraction operations and some quantum image transformations, the feature points could be extracted by comparing and thresholding the gradients of the pixels. Different methods of computing the pixel gradient and different thresholds can be realized under this quantum framework. The

This work is supported in part by the National High-tech R&D Program of China (863 Program) under Grants 2012AA01A301 and 2012AA010901, and it is partially supported by National Science Foundation China (NSFC 61103082, 61202333, and CPSF 2012M520392). Moreover, it is a part of Innovation Fund Sponsor Project of Excellent Postgraduate Student(B120601 and CX2012A002).

Y. Zhang (✉) · K. Lu · K. Xu
Science and Technology on Parallel and Distributed Processing Laboratory, College of Computer,
National University of Defense Technology, Changsha 410073, China
e-mail: zhangyinudt@nudt.edu.cn

K. Lu
e-mail: kailu@nudt.edu.cn

K. Xu
e-mail: kaixu@nudt.edu.cn

Y. Gao
College of Electronic Science and Engineering, National University of Defense Technology,
Changsha 410073, China
e-mail: yhgao@nudt.edu.cn

R. Wilson
Department of Computer Science, University of York, York YO10 5GH, UK
e-mail: richard.wilson@york.ac.uk

feature points extracted from quantum image can be used to construct quantum graph. Our work bridges the gap between quantum image processing and graph analysis based on quantum mechanics.

Keywords Quantum image · Feature extraction · Quantum adder · Quantum image transformation

1 Introduction

Image processing is an important branch of computer science, which has been widely used in many real-world applications such as biochemical, satellite navigation, and information retrieving [1]. With the recent development of image sensing techniques and the increasing size of image datasets, many traditional methods of digital image processing cannot achieve good accuracy as well as an acceptable scalability.

Since the first discussion of quantum computation by Feynman in 1982 [2], quantum information processing has been extensively investigated in the past decades. Compared with classical computation, quantum computation shows many amazing properties via utilizing quantum mechanics to represent and process information, such as quantum superposition, quantum entanglement, and quantum parallel computing. Some milestones of quantum research, especially the quantum integer factoring algorithm [3] and the quantum search algorithm [4], motivate researchers to use quantum mechanics to cope with more complex problems in the field of information processing.

Quantum image processing has proved to be very effective in the last decade. Several quantum image models have been designed to represent the image information including qubit lattice [5], Entangled Image [6], Real Ket [7], flexible representation of quantum images (FRQI) [8], and the novel enhanced quantum representation of digital images (NEQR) [9]. Meanwhile, many methods based on these models have been proposed to perform some simple processing for quantum images [10–20]. However, in general, quantum image processing is still in its infancy because most methods still only focuses on image storage and some image preprocessing tasks that are far from image processing, such as context analysis, pattern recognition, and image classification. One of the reasons is that there has been no quantum feature extraction algorithm based on the existing quantum image models so that none of the traditional recognition and classification methods based on feature points [21] can be leveraged to design a quantum counterpart algorithms for quantum images.

In this paper, a quantum feature extraction framework is proposed based on the novel enhanced quantum image model NEQR [9]. Because the color information of the pixels is stored in the basis state of a qubit sequence in the model NEQR, the quantum image addition and subtraction operations can be done flexibly via a proposed quantum full adder. And then, the gradients of all the pixels can be computed simultaneously via a sequence of quantum arithmetic operations. All the feature points can be extracted from the quantum image through setting a certain gradient threshold. This framework gives a general method to extract feature points for quantum images. The simple neighborhood mask [22] is used as an instance to show the procedure of feature point extraction in detail. In this paper, we only focus on the quantum information processing for the grayscale images.

The rest of this paper is organized as follows: the related works are discussed in Sect. 2 to introduce the development on quantum image processing. Section 3 describes the chosen quantum image model NEQR and discusses some important quantum image transformations based on this model. The proposed framework is presented in detail, and the complexity is analyzed in Sect. 4. Finally, conclusions and possible future research tracks are given in Sect. 5.

2 Related work

During the last decade, quantum image processing has been investigated extensively including quantum image models and quantum algorithms for some primary image processing tasks.

Qubit lattice, which was designed in 2002 [5], uses one qubit to store one pixel in the image, and the quantum amplitude of every qubit represents the color information of the relative pixel. This is the first image representation model using a quantum system. Through using the quantum entanglement to improve qubit lattice, Venegas-Andraca S.E. et al proposed another quantum image model, Entangled Image [6], which could use the relationship of some pixels to represent some shapes in the image. However, these two models do not utilize the quantum superposition so that the powerful quantum parallel computing cannot be used. Therefore, there are few efficient quantum algorithms based on the two models to do the quantum image processing.

Real Ket is the first quantum image model, which uses quantum superposition to store image information [7]. This model performs image quartering iteratively and builds a balanced quadtree for all the pixels. In the quantum image, every pixel is represented as a basis state of a four-dimensional qubit sequence. Because the quantum image in the Real Ket model is not a two-dimensional pixel matrix, the neighborhood information of the original image is destroyed so that the image processing tasks such as local feature extraction and edge detection cannot be done for the images stored in Real Ket.

Compared with Real Ket, the flexible representation of quantum images (FRQI) can store the two-dimensional position information of all the pixels. FRQI, which was designed by Le et al. in 2009 [8], uses a two-dimensional qubit sequence to represent the position of each pixel in the Cartesian coordinates while a qubit which is entangled with the position qubit sequence is used to represent the gray scale of the corresponding pixel. As the most popular quantum image model by now, many quantum image processing algorithms have been proposed based on FRQI including image preprocessing [10–15] and image watermarking algorithms [16–19]. However, FRQI uses only one qubit to represent the gray scales of the pixels so that complex color operations cannot be done flexibly. Therefore, it is quite difficult to extract feature points from the quantum images in the model FRQI.

Through improving the strategy to store the gray scale of the pixels, a novel enhanced quantum representation model for digital images (NEQR) was designed by our group [9]. The quantum images are the tensor product of two kinds of qubit sequences, which are used to represent the position and color information, respectively, in this model. Moreover, many complex color operations can be done for the

quantum image [9,20]. Therefore, NEQR will be the most suitable quantum image model to design feature extraction algorithms.

3 Flexible image transformations based on NEQR

Through comparing all the existing quantum image models, it is found that the model NEQR outperforms others on accessing the information of the neighborhood pixels and doing geometric and color transformations flexibly; it is the best choice to be the fundamental model to design the feature extraction framework. This section commences by a brief introduction of NEQR, and then some important image transformations that are at the core of the proposed framework will be discussed.

3.1 Quantum image model NEQR

In general, the pixels in a digital image have two kinds of information, namely position information and color information. In the quantum image model NEQR, these two kinds of information are individually stored in a two-dimensional qubit sequence. For an image with size $2^m \times 2^n$, we need to represent the X -axis and Y -axis coordinates by using two entangled qubit sequences with length m and n , respectively. Meanwhile, for the general grayscale images with gray range $[0, 2^q - 1]$, a q -length qubit sequence is needed to store the gray scale of pixels. The whole model is the tensor product of these three-qubit sequences that are entangled so that all the pixels can be stored and processed simultaneously.

(1) shows the expression of an NEQR image [9]. To store all the information, $m + n + q$ qubits are needed to construct the quantum image.

$$\begin{aligned} |I\rangle &= \frac{1}{\sqrt{2^{m+n}}} \sum_{Y=0}^{2^m-1} \sum_{X=0}^{2^n-1} |f(Y, X)\rangle |Y\rangle |X\rangle \\ &= \frac{1}{\sqrt{2^{m+n}}} \sum_{Y=0}^{2^m-1} \sum_{X=0}^{2^n-1} \bigotimes_{i=0}^{q-1} |C_{YX}^i\rangle |Y\rangle |X\rangle \end{aligned} \quad (1)$$

where $f(Y, X) = C_{YX}^{q-1} C_{YX}^{q-2} \cdots C_{YX}^1 C_{YX}^0$, $C_{YX}^k \in [0, 1]$, $f(Y, X) \in [0, 2^q - 1]$.

3.2 Geometric transformations for NEQR images

For the quantum images in the model NEQR, the quantum circuits of the geometric transformations consist of a sequence of unitary quantum gates on the position qubit sequence. Because every pixel is represented as a basis state of the quantum superposition, the position transformation will be computed simultaneously for all the pixels in the image. NEQR uses the similar method to store the position information with the model FRQI; therefore, the geometric transformations based on FRQI [10] and

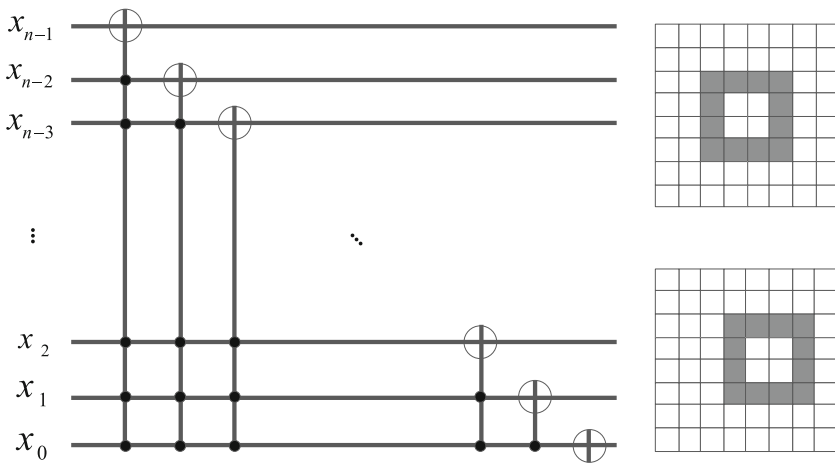


Fig. 1 **a** Quantum circuit of the operation S_{x+} for an NEQR image. **b** An example image and its transformed result

NEQR are same. In this subsection, we only give a brief discussion on the cycle shift operation, which will be used in the proposed feature extraction framework.

In order to utilize the neighborhood information to compute the gradients for all the pixels, the cycle shift transformation is used. For a two-dimensional digital image, the cycle shift operations on X -axis and Y -axis are symmetric and similar. Therefore, in this paper, the quantum operation S_{x+} is discussed as an example.

S_{x+} makes all the pixels move to the right position and adds one to its X -axis coordinate (For the edge pixels of the image, this operation is cycle. That is to say, during the operation S_{x+} , the pixels located at the right edges will move to the left edge in the transformed image. While the addition is also a cycle addition with module 2^n . Then, we will not consider the pixels in the edges as a special case). Then, the transformation of the quantum image is shown in (2), and the unitary matrix of S_{x+} is given in (3).

$$|I\rangle = \frac{1}{2^n} \sum_{Y=0}^{2^n-1} \sum_{X=0}^{2^n-1} |f(Y, X)\rangle |YX\rangle$$

$$\xrightarrow{S_{x+}} |I'\rangle = \frac{1}{2^n} \sum_{Y=0}^{2^n-1} \sum_{X=0}^{2^n-1} |f(Y, X)\rangle |Y\rangle |(X+1) \bmod 2^n\rangle \quad (2)$$

$$S_{x+} = \begin{bmatrix} \mathbf{0}^T & 1 \\ I_{2^n-1} & \mathbf{0} \end{bmatrix} \quad (3)$$

Figure 1 depicts the quantum circuit of the operation S_{x+} on the qubit sequence of the X -axis coordinate. According to the discussion in [10], it is reported that the quantum operation S_{x+} could be constructed by using no more than $O(n^2)$ Toffoli gates [23], it means the computation complexity of this operation is $O(n^2)$.

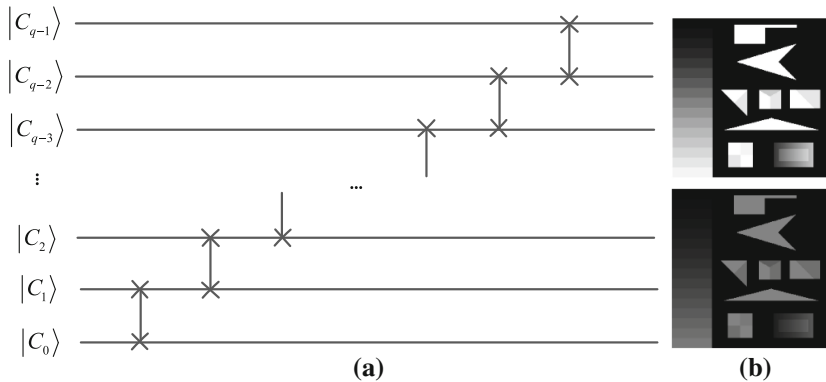


Fig. 2 **a** Quantum circuit of the halving operation U_H . **b** Example image and its transformed result

3.3 Color transformations for NEQR images

For the NEQR images, many complex color transformations can be done via utilizing the qubit sequence to represent the color information. In [9], some kinds of color operations were discussed based on NEQR such as the gray-range halving operation and the bi-valuing operation. In order to design the feature extraction algorithm, three kinds of color operations are discussed in this subsection.

The first color operation is the complement operation U_C , which is very important for the design of quantum image subtraction operation. This operation will make all the gray scales of the pixels in the image change to the complement values on 2^q . For the color qubit sequence of the quantum image, quantum NOT gates will be operated on all the qubits in the sequence in this operation. The expression and the quantum circuit of U_C were discussed in [9]. Meanwhile, it was reported that the time complexity is no more than $O(q)$ for an image with gray range $[0, 2^q - 1]$.

The second operation is the halving operation U_H . This operation will make the gray scale of all the pixels be reduced by half. As this image operation, the gray range is also reduced. For a quantum image in the model NEQR, this operation will make all the qubits in the color sequence cycle shift down. (4) shows the transformation of the quantum operation U_H . To realize this task, $q - 1$ simple quantum swap gates are used to build the quantum circuit as shown in Fig. 2. Therefore, the time complexity of the operation U_H is also no more than $O(q)$.

$$\begin{aligned}
 U_H(|I\rangle) &= U_H \left(\frac{1}{2^n} \sum_{Y=0}^{2^n-1} \sum_{X=0}^{2^n-1} |f(Y, X)\rangle |Y\rangle |X\rangle \right) \\
 &= U_H \left(\frac{1}{2^n} \sum_{Y=0}^{2^n-1} \sum_{X=0}^{2^n-1} \bigotimes_{i=0}^{q-1} |C_{YX}^i\rangle |Y\rangle |X\rangle \right)
 \end{aligned}$$

$$\begin{aligned}
&= \frac{1}{2^n} \sum_{Y=0}^{2^n-1} \sum_{X=0}^{2^n-1} \left(\left| C_{YX}^0 \right\rangle \bigotimes_{i=0}^{q-2} \left| C_{YX}^{i+1} \right\rangle |Y\rangle |X\rangle \right) \\
&= \frac{1}{2^n} \sum_{Y=0}^{2^n-1} \sum_{X=0}^{2^n-1} \left| C_{YX}^0 \right\rangle |f(Y, X)/2\rangle |Y\rangle |X\rangle
\end{aligned} \quad (4)$$

The third one is the classification operation U_T for all the pixels in the image. Via setting a threshold T , all the pixels with gray scale less than the threshold belong to one group and the left are in the other group.

To store the result of the classification, we need an auxiliary qubit, which should be entangled with the image, and it will be set to $|0\rangle$ in the initial as shown in (5).

$$|I\rangle |0\rangle = \frac{1}{2^n} \sum_{Y=0}^{2^n-1} \sum_{X=0}^{2^n-1} |f(Y, X)\rangle |YX\rangle |0\rangle \quad (5)$$

The choice of the threshold is very important in this operation, which is relative to the quantum circuit and the time complexity. In general, when a threshold T is chosen, the auxiliary qubit corresponding to all the pixels with gray scale no less than T should turn around, and the transformation of the operation U_T is shown as (6).

$$\begin{aligned}
U_T(|I\rangle |0\rangle) &= U_T \left(\frac{1}{2^n} \sum_{Y=0}^{2^n-1} \sum_{X=0}^{2^n-1} |f(Y, X)\rangle |YX\rangle |0\rangle \right) \\
&= \frac{1}{2^n} \left(\sum_{f(Y,X) \geq T} |f(Y, X)\rangle |YX\rangle |1\rangle + \sum_{f(Y,X) < T} |f(Y, X)\rangle |YX\rangle |0\rangle \right)
\end{aligned} \quad (6)$$

To simplify the quantum circuit, the minimization of Boolean expressions [24] can be used. To be simple, for an image with gray range $[0, 2^q - 1]$, the threshold which is equal to powers of 2 is often chosen, and it is easy to design the quantum circuit. For example, if the threshold is 2^{q-2} , the highest two-color qubits are needed to be the controllers, and the quantum circuit is shown in Fig. 3.

For the worst case, all the qubits in the color sequence are needed to be the controllers of the auxiliary qubit. That is to say, we need q -Cnot quantum gates in the quantum circuit. According to the discussion of the time complexity of shift operation in [10], we can conclude that the time complexity of the classification operation U_T is no more than $O(q^2)$.

4 Quantum feature extraction framework

In the previous section, the quantum image model NEQR and some important image operations are discussed. Based on these quantum image transformations, the feature

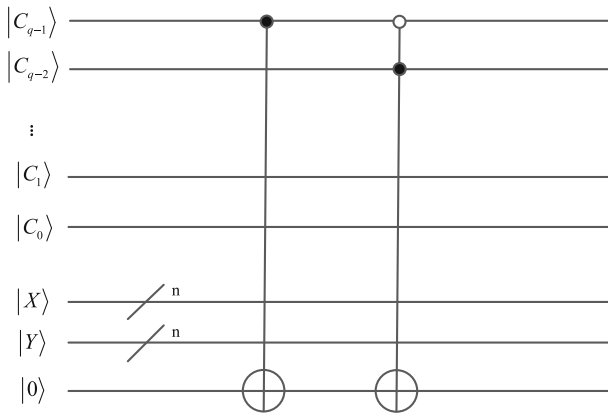


Fig. 3 Quantum circuit of the quantum operation U_T . Here, $T = 2^{q-2}$

extraction framework is proposed. In this paper, we aim to compute corner points using a gradient-based method [25]. Therefore, the first problem is how to compute the gradients for all the pixels in the quantum image.

4.1 Quantum image addition and subtraction operations

In this subsection, we focus on how to make the addition and subtraction operations of two quantum images in the model NEQR. For the image addition operation of two images, the pixels of the result image have the arithmetic additions of the gray scales of the corresponding pixels in the two images. A similar method is applied to the subtraction operation. Therefore, how to use the two-color qubit sequences to obtain the arithmetic result will be discussed at first.

Assume that the two quantum images $|I_A\rangle$ and $|I_B\rangle$ are both with size $2^n \times 2^n$ and with gray range $[0, 2^q - 1]$. The two image expressions are shown in (7).

$$\begin{aligned} |I_A\rangle &= \frac{1}{2^n} \sum_{YX=0}^{2^{2n}-1} |A_{YX}\rangle |YX\rangle \\ |I_B\rangle &= \frac{1}{2^n} \sum_{YX=0}^{2^{2n}-1} |B_{YX}\rangle |YX\rangle \end{aligned} \quad (7)$$

where $|A_{YX}\rangle = \bigotimes_{i=0}^{q-1} |a_i\rangle$ and $|B_{YX}\rangle = \bigotimes_{i=0}^{q-1} |b_i\rangle$.

Firstly, we discuss the quantum image addition operation. Suppose the result quantum image is $|I_C\rangle$ shown in (8). It is known that for every pixel (Y, X) in the result image, the gray scale C_{YX} is equal to the sum of A_{YX} and B_{YX} .

$$|I_C\rangle = \frac{1}{2^n} \sum_{YX=0}^{2^{2n}-1} |C_{YX}\rangle |YX\rangle = \frac{1}{2^n} \sum_{YX=0}^{2^{2n}-1} |A_{YX} + B_{YX}\rangle |YX\rangle \quad (8)$$

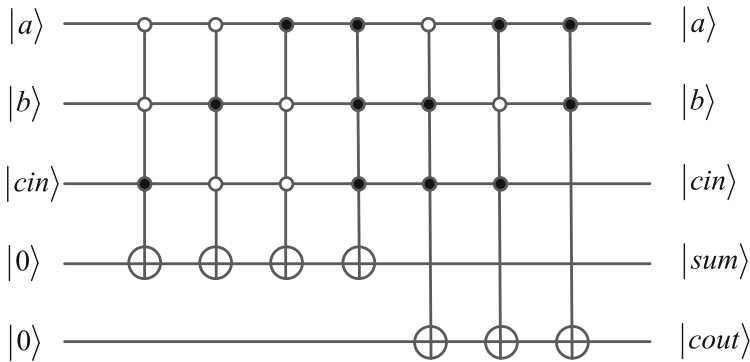


Fig. 4 Quantum circuit of 1-qubit quantum full adder

Because $A_{YX}, B_{YX} \in [0, 2^q - 1]$, it is known that $C_{YX} \in [0, 2^{q+1} - 1]$, and therefore, $q + 1$ qubits are needed to store the result, that is to say, $|C_{YX}\rangle = \bigotimes_{i=0}^q |c_i\rangle$.

Then, a quantum full adder is designed to compute the arithmetic result $|C_{YX}\rangle = |A_{YX} + B_{YX}\rangle$ of the two quantum states $|A_{YX}\rangle$ and $|B_{YX}\rangle$.

An 1-bit full adder has three inputs (a , b , the two input bits; cin , the previous carry bit) and two outputs (sum , the result of the addition; $cout$, the current carry bit). Analogously, we can design the quantum counterpart with the similar method. In the initial, we set $|0\rangle$ to the output qubits. Then, we use the quantum circuit as shown in Fig. 4 to compute the arithmetic operation. There are totally 6 3-Cnot gates and 1 2-Cnot gate in this quantum circuit, and the quantum operation can be expressed as (9).

$$|a\rangle |b\rangle |cin\rangle |0\rangle |0\rangle \xrightarrow{1-ADD} |a\rangle |b\rangle |cin\rangle |sum\rangle |cout\rangle \quad (9)$$

By using q 1-qubit quantum full adders, the q -qubit quantum full adder can be constructed. Figure 5 demonstrates the construction of the q -qubit full adder where $|A\rangle = \bigotimes_{i=0}^{q-1} |a_i\rangle$ and $|B\rangle = \bigotimes_{i=0}^{q-1} |b_i\rangle$ are the input numbers and $|C\rangle = \bigotimes_{i=0}^q |c_i\rangle$ is the result and $|F\rangle = \bigotimes_{i=0}^{q-1} |f_i\rangle$ are the auxiliary qubits. It is known that q auxiliary qubits are needed in the q -qubit full adder. Similarly, we set $|0\rangle$ to the output qubits $|C\rangle$ and $|F\rangle$ in the initial.

Because the whole procedure of this quantum arithmetic operation is consisted of q 1-qubit full adders which use 7 quantum gates individually, the time complexity of the q -qubit full adder is approximately $O(q)$ by using q auxiliary qubits. Therefore, for two quantum images $|I_A\rangle$ and $|I_B\rangle$, the quantum image addition operation can be done via a q -qubit full adder on the two-color qubit sequences of the two images to obtain the result image $|I_C\rangle$ as defined in (10).

$$|I_C\rangle = qADD(|I_A\rangle, |I_B\rangle) \quad (10)$$

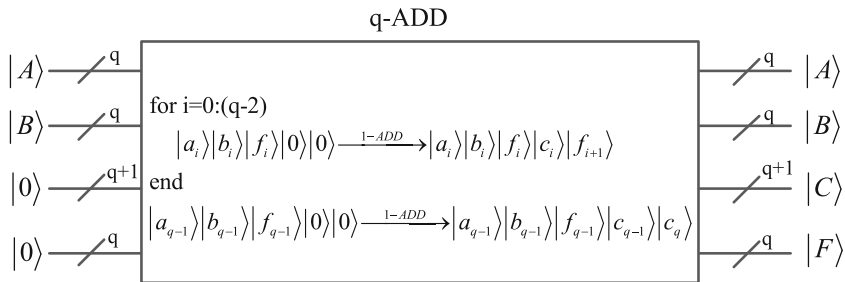


Fig. 5 Quantum circuit of q -qubit full adder. The whole procedure is consisted of q 1-qubit quantum full adders

In actual, the arithmetic subtraction is similar to the addition operation. To compute the result of the subtraction of two images $|I_A\rangle$ and $|I_B\rangle$, we can make an image complement operation on $|I_B\rangle$ to get $|I_{\bar{B}}\rangle$ ($|I_{\bar{B}}\rangle = U_C |I_B\rangle$) and then compute the summation of $|I_A\rangle$ and $|I_{\bar{B}}\rangle$. At last, the highest qubit of the color sequence of the addition image needs to turn around to obtain the final result image $|I_C\rangle$. Because the whole procedure is easy to realize after discussing the quantum image addition, we do not give the detail quantum circuit of the quantum image subtraction. However, it is worth noting that when $A_{YX}, B_{YX} \in [0, 2^q - 1]$, $C_{YX} = A_{YX} - B_{YX} \in [-(2^q - 1), 2^q - 1]$. We also need $q + 1$ qubits to store the gray scale of the pixels of the result image. When the highest qubit is $|0\rangle$, it implies that $A_{YX} \geq B_{YX}$. Otherwise, $A_{YX} < B_{YX}$. If we neglect the highest qubit, the operation will compute the absolute value of the subtraction of A_{YX} and B_{YX} . Therefore, for two quantum images $|I_A\rangle$ and $|I_B\rangle$, the quantum image subtraction operation can obtain the result image $|I_C\rangle$ as defined in (11).

$$|I_C\rangle = qSUB(|I_A\rangle, |I_B\rangle) \quad (11)$$

In [26], a more efficient quantum full adder and subtractor was proposed. Less quantum gates need to be used in this method. However, this kind of quantum full adder stores the result in the input qubits. If we use this kind of quantum full adder to do image addition operation, it means that we could obtain the result image, but the information of one of the input images is discarded. In the following framework, every input image will be used multi-times to do some image addition and subtraction operations. Therefore, we consider that the efficient method is not suitable for our framework.

4.2 The framework of quantum feature extraction

In this paper, the feature points which will be extracted from the images are the corner pixels that have different gray scale with the neighborhood pixels in all directions. In general, the gradient of every direction of one pixel is used to represent the degree of the difference from its neighbors. Theoretically, the more neighborhood information is used, the computation of the gradient is more complex, and the extracted features are more effective to represent the local properties of the image. The whole framework will be divided into four steps as shown in Fig. 6.

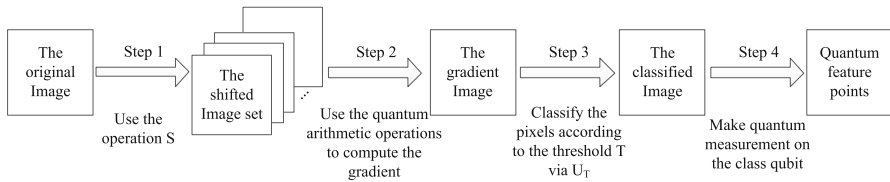


Fig. 6 Workflow of the feature extraction framework based on quantum image

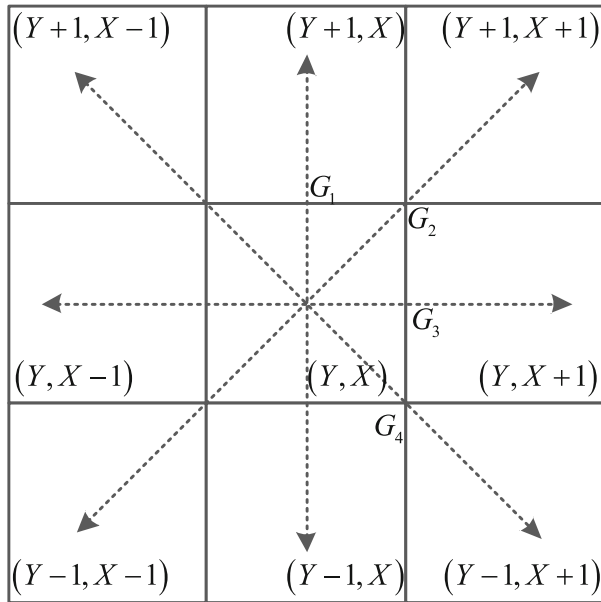


Fig. 7 3×3 neighborhood pixels of pixel (Y, X) . G_1 - G_4 are the subgradients of the four common orientations in this mask

One simple method to compute the gradient of the pixels is the 1-order differential coefficient, which will use the 3×3 neighborhood of the pixel shown as Fig. 7 [22]. Many important methods to compute the pixel gradients have been discussed based on this kind of mask such as zero cross [22], Sobel [27], SUSAN [28], and Harris [29].

Then, we will give the framework of the quantum feature extraction based on the quantum image model NEQR. Enough auxiliary qubits are supplied to do the whole procedure.

Step 1. Obtain the eight shifted quantum images via some certain cycle shift operations on $|I_{YX}\rangle$. And now, we have the quantum image set as

$$\{|I_{YX}\rangle, |I_{Y-1X}\rangle, |I_{Y+1X}\rangle, |I_{Y-1X-1}\rangle, |I_{YX-1}\rangle, |I_{Y+1X-1}\rangle, |I_{Y-1X+1}\rangle, |I_{YX+1}\rangle, |I_{Y+1X+1}\rangle\}$$

In this step, eight shifted images are computed and stored in the quantum states. This is an important difference between our framework and the traditional methods. In

the latter, only one temporal image is used, and the neighbor pixels are not stored separately.

Step 2. Choose the method of computing the gradient of the pixels. To obtain the 1-order differential coefficient of the image, a sequence of quantum image addition and quantum image subtraction operations are used on the relative images in the quantum image set. The detail procedure depends on the chosen method to compute the gradient. At last, the gradient of every pixel of the image can be computed via the quantum image halving operation on the result image of the arithmetic procedure. Then, we use the famous method, zero cross [22], to exemplify this step of the framework.

In the zero-cross method, the subgradients of four directions of every pixel need to be computed as shown in Fig. 7. And for the pixel (Y, X) , the gradients are computed based on its 3×3 neighborhood information as (12).

$$\begin{aligned} G_1 &= |2C_{YX} - (C_{Y+1X} + C_{Y-1X})| / 2 \\ G_2 &= |2C_{YX} - (C_{Y+1X+1} + C_{Y-1X-1})| / 2 \\ G_3 &= |2C_{YX} - (C_{YX+1} + C_{YX-1})| / 2 \\ G_4 &= |2C_{YX} - (C_{Y+1X-1} + C_{Y-1X+1})| / 2 \end{aligned} \quad (12)$$

where C_{YX} is the gray scale of the pixel (Y, X) .

For every direction, we need two quantum image addition, one quantum image subtraction, and one quantum image halving operation to finish the computation of the gradient. The procedure of the computation of all the four subgradients for all the pixels in the image is shown in (13). There are totally 5 $qADD$ operations, 4 $qSUB$ operations, and 4 U_H operations in this procedure.

$$\begin{aligned} |\varphi_0\rangle &= qADD(|I_{YX}\rangle, |I_{YX}\rangle), \\ |\varphi_1\rangle &= qADD(|I_{Y+1X}\rangle, |I_{Y-1X}\rangle), & |\varphi_2\rangle &= qSUB(|\varphi_0\rangle, |\varphi_1\rangle), \\ |\varphi_3\rangle &= qADD(|I_{Y+1X+1}\rangle, |I_{Y-1X-1}\rangle), & |\varphi_4\rangle &= qSUB(|\varphi_0\rangle, |\varphi_3\rangle), \\ |\varphi_5\rangle &= qADD(|I_{YX+1}\rangle, |I_{YX-1}\rangle), & |\varphi_6\rangle &= qSUB(|\varphi_0\rangle, |\varphi_5\rangle), \\ |\varphi_7\rangle &= qADD(|I_{Y+1X-1}\rangle, |I_{Y-1X+1}\rangle), & |\varphi_8\rangle &= qSUB(|\varphi_0\rangle, |\varphi_7\rangle), \\ |G_1\rangle &= U_H |\varphi_2\rangle, & |G_2\rangle &= U_H |\varphi_4\rangle, \\ |G_3\rangle &= U_H |\varphi_6\rangle, & |G_4\rangle &= U_H |\varphi_8\rangle. \end{aligned} \quad (13)$$

Step 3. Make the pixel classification operation U_T based on a threshold T .

The choice of threshold T is very important in the feature extraction methods. Two strategies are often used to choose threshold in the traditional feature extractors, i.e., user-defined threshold and adaptive one. The construction of the quantum circuit of the detailed quantum operation U_T in this framework depends on the threshold value. So the adaptive threshold is not suitable for our framework. Therefore, in our method, we need to set a fixed threshold before extracting features.

According to the property of the feature points, it is known that the gradients of all the directions of the feature points in the image should be quite different with the neighborhood. Therefore, some auxiliary qubits are needed to record the result whether the subgradient of every direction is larger than the threshold.

If the zero-cross method is used, there are four subgradients of every pixel. Therefore, four qubits $\{|z_i\rangle \mid 1 \leq i \leq 4\}$ are used to store the classification result of the pixel classification operation on the four result images $\{|G_i\rangle \mid 1 \leq i \leq 4\}$ of *Step 2*.

Step 4. After *Step 3*, the useful part of the whole quantum system is the entanglement of the position qubit sequence and the four classification result qubits $|Z\rangle$ as shown in (14).

$$|\Psi\rangle = \frac{1}{2^n} \sum_{YX=0}^{2^{2n}-1} |YX\rangle \otimes |Z\rangle \quad (14)$$

where $|Z\rangle = \bigotimes_{i=1}^l |z_i\rangle$ is the qubit sequence to store the classification result of every pixel. The length l depends on the number of the direction we have computed in *Step 2*.

It is claimed that the feature points are the pixels that have different gray scale with the neighborhood pixels in all directions. It means that a pixel can be considered as a feature only when every classification result $|z_i\rangle$ is equal to $|1\rangle$.

Then, a quantum measurement will be operated on this quantum sequence. When we observe that $|Z\rangle = |11 \cdots 1\rangle$, the quantum system will be collapsed into a new quantum superposition, which is consisted of all the feature points we extract from the image as shown in (15).

$$|\Omega\rangle = a \sum_{\substack{0 \leq Y \leq 2^{2n}-1 \\ 0 \leq X \leq 2^{2n}-1 \\ |Z_{YX}\rangle = |11 \cdots 1\rangle}} |YX\rangle \quad (15)$$

In order to avoid repeated experiments, the Grover technique [4] can be utilized to change the quantum amplitudes of the expected result so that we can observe $|Z\rangle = |11 \cdots 1\rangle$ in a probability of approximate 100 % for a quantum measurement.

It is worth to note that the whole framework will obtain a quantum superposition of all the features of a quantum image while if we need to read out which pixels are features from the superposition, the whole measurement will take $O(2^{2n})$ so that the measurement time will dominate. However, feature extraction is just one step of image preprocessing and usually we do not focus on which pixels are features. Many complex operations will work on the feature superposition to obtain more significant information. For example, we can utilize the quantum counting algorithm in [30] to obtain the number of the features. Therefore, we do not need to consider the measurement time to read out features.

4.3 Algorithm analysis

In this subsection, we will discuss the time complexity of the framework of the proposed quantum feature extraction.

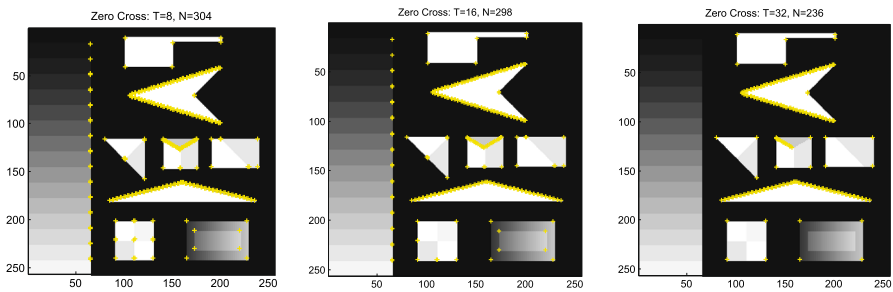


Fig. 8 Feature extraction result from the test image. The three figures give the result by using the zero-cross method. T denotes the threshold. N gives the number of the extracted feature points

For the first step, several times of quantum cycle shift operations are used to obtain the transformed quantum image set. Because only 8 images are needed, this step will cost approximately $O(n^2)$.

Step 2 will use some quantum image addition and subtraction operations to compute the gradients of all the pixels in the image. As the discussion in Sect. 4.1, one quantum image addition will cost about $O(q)$. And the complexity of the quantum image subtraction and the image halving operation are also $O(q)$. Therefore, the time complexity of *Step 2* is about $O(q)$.

For every subgradient of the directions of the pixels, one quantum pixel classification operation will be done in *Step 3*. Therefore, this step will cost no more than $O(q^2)$.

After all, if we neglect the time cost of quantum measurement, the time complexity of the whole procedure is about $O(n^2 + q^2)$ at worst case to extract the feature points of an image with size $2^n \times 2^n$ and gray range $[0, 2^q - 1]$.

As the discussion above, the chosen method to compute the gradient and the chosen threshold are the two important aspects on the performance of the feature extraction algorithm. Therefore, for the test image [28], the feature extraction results using the zero-cross method and different thresholds ($T = 8, 16, 32$) are shown in Fig. 8. Because we only use the 3×3 neighborhood information in the simple zero-cross method, it is inevitable that there are some wrong features in the result images.

5 Conclusion

The researches of quantum image processing are still primary because of the lack of the feature extraction algorithms based on the existing quantum images. Therefore, the high-level image processing tasks are difficult to be processed such as pattern recognition and image classification.

In this paper, a quantum feature extraction framework is proposed based on the quantum image in the model NEQR. Because qubit sequences are used to store the position and color information in the model NEQR, many complex geometric and color transformations can be operated, which are the fundamental parts of the proposed framework. Via comparing the gradients of the pixels and the setting threshold, all the

feature points will be extracted and stored in a quantum superposition via a quantum procedure with approximate complexity $O(n^2 + q^2)$ for images with size $2^n \times 2^n$ and gray range $[0, 2^q - 1]$.

Graph is an important abstract structure in image understanding. How to utilize quantum mechanics to analysis graph has been investigated extensively [31–35]. Feature extraction is a common bridge between image and graph [36]. Meanwhile, quantum walk is an important tool to analyze graphs. For continuous-time quantum walk on a graph [33], the quantum state is the superposition of all the nodes of the graph, which is just the superposition of all the feature points in the relative image, and is just the output of our framework.

Therefore, the proposed framework connects the researches of quantum image processing and graph analysis based on quantum computation. By now, one entire and available quantum system for image processing have been demonstrated, which will work on a quantum computer in the future.

Acknowledgments The authors appreciate the kind comments and professional criticisms of the anonymous reviewer. This has greatly enhanced the overall quality of the manuscript and opened numerous perspectives geared toward improving the work. This work is supported in part by the National High-tech R&D Program of China (863 Program) under Grants 2012AA01A301 and 2012AA010901, and it is partially supported by National Science Foundation China (NSFC 61103082, 61202333 and CPSF 2012M520392). Moreover, it is a part of Innovation Fund Sponsor Project of Excellent Postgraduate Student (B120601 and CX2012A002).

References

1. Gonzalez, R.C., Woods, R.E., Eddins, S.L.: Digital Image Processing. Publishing House of Electronics Industry, Beijing (2002)
2. Feynman, R.: Simulating physics with computers. *Int. J. Theor. Phys.* **21**, 467–488 (1982)
3. Shor, P.W.: Algorithms for quantum computation: discrete logarithms and factoring. In: *Proceeding of 35th Annual Symposium Foundations of Computer Science*, pp. 124–134. IEEE Computer Society Press, Los Almitos, CA (1994)
4. Grover, L.: A fast quantum mechanical algorithm for database search. In: *Proceedings of the 28th Annual ACM Symposium on the Theory of Computing*, pp. 212–219 (1996)
5. Venegas-Andraca, S.E., Bose, S.: Storing, processing and retrieving an image using quantum mechanics. In: *Proceeding of the SPIE Conference Quantum Information and Computation*, pp. 137–147 (2003)
6. Venegas-Andraca, S.E., Ball, J.L., Burnett, K., Bose, S.: Processing images in entangled quantum systems. *Quantum Inf. Process.* **9**, 1–11 (2010)
7. Latorre, J.I.: Image compression and entanglement. [arXiv:quant-ph/0510031](https://arxiv.org/abs/quant-ph/0510031) (2005)
8. Le, P.Q., Dong, F., Hirota, K.: A flexible representation of quantum images for polynomial preparation, image compression, and processing operations. *Quantum Inf. Process.* **10**(1), 63–84 (2011)
9. Zhang, Y., Lu, K., Gao, Y., Wang, M.: NEQR: a novel enhanced quantum representation of digital images. *Quantum Inf. Process.* (2013). doi:[10.1007/s11128-013-0567-z](https://doi.org/10.1007/s11128-013-0567-z)
10. Le, P.Q., Iliyasu, A.M., Dong, F., Hirota, K.: Strategies for designing geometric transformations on quantum images. *Theor. Comput. Sci.* **412**, 1406–1418 (2011)
11. Le, P.Q., Iliyasu, A.M., Dong, F., Hirota, K.: Efficient color transformations on quantum images. *J. Adv. Comput. Intell. Intell. Informa.* **15**(6), 698–706 (2011)
12. Bo, S., Le, P.Q., Iliyasu, A.M., etc.: A multi-channel representation for images on quantum computers using the RGB α color space. In: *Proceedings of the IEEE 7th International Symposium on Intelligent Signal Processing*, pp. 160–165 (2011)
13. Fei, Y., Le, P.Q., Iliyasu, A.M., Bo, S.: Assessing the similarity of quantum images based on probability measurements. In: *IEEE Congress on Evolutionary Computation*, pp. 1–6 (2012)

14. Jiang, N., Wu, W., Wang, L.: The quantum realization of Arnold and Fibonacci image scrambling. *Quantum Inf. Process.* **13**(5), 1223–1236 (2014)
15. Caraiman, S., Manta, V.I.: Histogram-based segmentation of quantum images. *Theor. Comput. Sci.* **529**, 46–60 (2014)
16. Ilyasu, A.M., Le, P.Q., Dong, F., Hirota, K.: Watermarking and authentication of quantum images based on restricted geometric transformations. *Inf. Sci.* **186**, 126–149 (2012)
17. Zhang, W., Gao, F., Liu, B., Wen, Q., Chen, H.: A watermark strategy for quantum images based on quantum fourier transform. *Quantum Inf. Process.* doi:[10.1007/s11128-012-0423-6](https://doi.org/10.1007/s11128-012-0423-6) (2012)
18. Song, X., Wang, S., Liu, S., Abd El-Latif, A.A., Niu, X.: A dynamic watermarking scheme for quantum images using quantum wavelet transform. *Quantum Inf. Process.* **12**(12), 3689–3706 (2013)
19. Zhou, R., Wu, Q., Zhang, M., Shen, C.: Quantum image encryption and decryption algorithms based on quantum image geometric transformations. *Int. J. Theor. Phys.* **52**(6), 1802–1817 (2013)
20. Zhang, Y., Lu, K., Gao, Y., Xu, K.: A novel quantum representation for log-polar images. *Quantum Inf. Process.* doi:[10.1007/s11128-013-0587-8](https://doi.org/10.1007/s11128-013-0587-8) (2013)
21. Edward, R., Drummond, T.: *Machine Learning for High-Speed Corner Detection*. Computer Vision—ECCV. Springer, Berlin (2006)
22. Marr, D., Hildreth, E.: Theory of edge detection. *Proc. R. Soc. Lond.* **B275**, 187–217 (1980)
23. Yang, G., Song, X., Hung, W., et al.: Group theory based synthesis of binary reversible circuits. *Lect. Notes Comput. Sci.* **3959**, 365–374 (2006)
24. Brayton, R.K., Sangiovanni-Vincentelli, A., McMullen, C., Hachtel, G.: *Logic Minimization Algorithms for VLSI Synthesis*. Kluwer, Dordrecht (1984)
25. Mehrotra, R., Sanjay, N., Nagarajan, R.: Corner detection. *Pattern Recognit.* **23**(11), 1223–1233 (1990)
26. Cheng, K., Tseng, C.: Quantum full adder and subtractor. *Electron. Lett.* **38**(22), 1343–1344 (2002)
27. Sobel, L.: *Camera Models and Machine Perception*. Stanford University, CA (1970)
28. Smith, S.M., Brady, J.M.: SUSAN—a new approach to low level image processing. *Int. J. Comput. Vis.* **23**(1), 45–78 (1997)
29. Harris, C., Stephens, M.: A combined corner and edge detector. In: *Proceedings of the 4th Alvey Vision Conference*, pp. 147–151 (1988)
30. Gilles, B., Høyer, P., Tapp, A.: Quantum counting. In: *Automata, Languages and Programming*, pp. 820–831. Springer, Berlin, Heidelberg (1998)
31. Qiang, X., Yang, X., Wu, J., Zhu, X.: An enhanced classical approach to graph isomorphism using continuous-time quantum walk. *J. Phys. A: Math. Theor.* **45**(4), 045305 (2012)
32. Douglas, B.L., Wang, J.B.: A classical approach to the graph isomorphism problem using quantum walks. *J. Phys. A: Math. Theor.* **41**(7), 075303 (2008)
33. Emms, D., Wilson, R.C., Hancock, E.R.: Graph matching using the interference of continuous-time quantum walks. *Pattern Recognit.* **42**(5), 985–1002 (2009)
34. Emms, D., Severini, S., Wilson, R.C., Hancock, E.R.: Coined quantum walks lift the cospectrality of graphs and trees. *Pattern Recognit.* **42**(9), 1988–2002 (2009)
35. Lu, K., Zhang, Y., Gao, Y., et al.: Approximate maximum common sub-graph isomorphism based on discrete-time quantum walk. In: *International Conference on Pattern Recognition* (2014)
36. Aziz, F., Wilson, R.C., Hancock, E.R.: Backtrackless walks on a graph. *IEEE Trans. Neural Netw. Learn. Syst.* **24**(6), 977–989 (2013)